PHYSICAL MODELLING OF PILE TIP DAMAGE ARISING FROM IMPACT DRIVING

Juliano A. Nietiedt, Centre for Offshore Foundation Systems, The University of Western Australia, Perth, Australia, +61 0415 081 891, juliano.nietiedt@research.uwa.edu.au

Mark F. Randolph, Centre for Offshore Foundation Systems, The University of Western Australia, Perth, Australia, mark.randolph@uwa.edu.au

Christophe Gaudin, Centre for Offshore Foundation Systems, The University of Western Australia, Perth, Australia, Christophe.gaudin@uwa.edu.au

James Doherty, Centre for Offshore Foundation Systems, The University of Western Australia, Perth, Australia, james.doherty@uwa.edu.au

Dan Kallehave, Ørsted Offshore, Gentofte, Denmark, dakal@orsted.dk

Jens Gengenbach, Ørsted Offshore, Hamburg, Germany, jenge@orsted.de

Avi Shonberg, Ørsted Offshore, London, UK, avish@orsted.co.uk

Keywords: extrusion buckling, pile tip damage, centrifuge tests, monopiles, pile driving

ABSTRACT

There have been a number of incidents worldwide where pile tip damage has occurred during pile driving, generally requiring costly remedial actions. The number of such occurrences has increased recently, consistent with the trend of increasing diameter tubular piles, which are increasingly thin-walled relative to the diameter, used to support offshore wind turbines either as monopiles or as part of a jacket structure. As the wind industry moves into new regions of the world, challenging soil conditions are becoming more common, in particular with increasing risks from embedded boulders or partially weathered soft rocks including chalk and limestone. Pile tip damage may occur as a rather abrupt tip 'crumpling', or as a more gradual progressive 'extrusion buckle'. Both are likely to be triggered by localised heterogeneous hard zones within the sediments, with the rate of growth determined by the stiffness of the surrounding soil matrix. The paper reports some results from a pilot series of centrifuge model tests where thin-walled piles were driven in flight into a sand bed containing thin layers of either 'gravel' (representing boulders of up to 30% of the pile diameter), or weakly cemented material. Tip damage varying from barely perceptible to rather extreme was triggered, resulting in increasing driving resistance and premature refusal.

INTRODUCTION

Over the last 30 years a series of well-documented case histories have been reported in which open-ended steel pipe piles have undergone gradual closure during driving into dense soils or soft rocks (Kramer 1996; Alm et al. 2004; Erbrich et al. 2010). This form of failure, where the pile tip becomes increasingly more distorted from the original circular shape, is commonly referred to as 'extrusion buckling'. Once the pile tip buckling starts the driving resistance increases, which may cause premature refusal, which means that the pile cannot be driven to the design depth. This may lead to significant problems for piles with significant tension requirements or where features such as weld beads or variations in pile wall thickness need to occur at a specific elevation. Complete or partial closure of the tip may also prevent subsequent construction work such as drilling out the soil plug to alleviate driving resistance or to install grouted insert piles.

The onset of buckling is governed by a number of factors:

- Pile geometry: The diameter (D), wall thickness (t) and hence the ratio (D/t) are the principal geometric parameters that control the potential to develop buckling.

- Initial imperfections: Small imperfections such as fabrication out-of-roundness of the pile cross-section or damage to the pile tip (as a dent) significantly decrease the buckling resistance of the pile and may trigger extrusion buckling.
- Soil heterogeneity: Variations in soil strength in planes normal to the pile axis or localized hard zones may induce initial distortion (ovalization) of the pile cross-section, which may initiate extrusion buckling.
- Soil and pile stiffness: Propagation of extrusion buckling can occur if the pile hoop-stiffness is significantly smaller than the soil cavity expansion stiffness.
- Dynamic effects: High dynamic tip stresses arising during impact driving of piles through weak rock may contribute to the initiation of local plasticity in the steel and some form of buckling (Stevens et al. 1982; Wiltsie et al. 1985).

Over the last decade there has been a trend of using ever larger diameter piles for anchoring floating systems offshore and founding wind turbines, although without corresponding increases in wall thickness, resulting in higher D/t ratios. The API (2002) guidelines are often used as the basis to choose acceptable pile tip D/t ratios. However, those guidelines were intended to avoid tip buckling due to excessive axial driving stresses rather than extrusion buckling, and they allow D/t ratios of 80 to 90 for piles of more than 3 m in diameter. This has increased the frequency of tip damage and extrusion buckling of piles used in the offshore wind industry, where piles of up to 7.5 m have been used, during driving into different sediments such as partially weathered mudstone, dense sands or weak limestone.

A research project is currently underway in the Centre for Offshore Foundation Systems at the University of Western Australia, with the aim to improve quantitative prediction of conditions where extrusion buckling may occur. This paper presents the results from an initial pilot study of centrifuge model tests where a total of nine piles were driven into dense sand, including through cemented sand and a boulder layer. Various degrees of pile tip damage and extrusion buckling were observed.

BACKGROUND – FIELD CASES AND ANALYSIS

The first well documented case of extrusion buckling was the Goodwyn A platform installed in the North West Shelf of Australia in the late 1980s, where 16 of the 20 driven primary piles (diameter of 2.65 m, D/t = 59) underwent extrusion buckling triggered by a very hard, 3-5 m thick calcarenite layer, present at a depth of 75 m (Kramer 1996; Erbrich et al. 2010) – see Fig. 1. In another case five out of eight piles (2.44 m diameter with D/t of 40) for the Valhall water injection platform in the North Sea reached premature refusal during driving into very dense sand with cone resistance of q_c ~ 80 MPa (Alm et al. 2004).

A numerical technique called BASIL (Buckled Adjusted Soil Installation Loading) (Barbour and Erbrich 1994; 1995; Erbrich et al. 2010) was developed to address this type of issue and has been used widely by industry (e.g. Erbrich et al. 2017; Finnie et al. 2019). In principle, initiation and propagation of extrusion buckling may also be modelled using conventional large deformation finite element techniques (Bakroon et al. 2018).

Pile tip damage and extrusion buckling initiation

In applications reported to date, extrusion buckling has been triggered within BASIL by assuming slight non-circularity of the pile tip, according to one of the buckling modes, although triggering as a result of heterogeneous soil conditions may also be implemented. Localised tip damage, which may occur during transport and offshore handling, or due to encountering a boulder or other localised strong material during installation, is another potential trigger. HSE (2001) explored this aspect and provided simple formulations to estimate the forces and pressures necessary to cause tip damage and buckling of pipes. The formulations are based on analytical and empirical solutions for structural elements (Bresse 1866; Timoshenko and

Gere 1961; Ellinas and Walker 1983). Aldridge et al. (2005) also considered the forces necessary to cause a small dent at the pile tip and the soil conditions where such damage would tend to propagate. The primary criterion for propagation is that the soil needs to be sufficiently stiff to overcome the (initially elastic) hoop stiffness of the steel. However, since the pile hoop-stiffness is inversely proportional to the cube of the D/t ratio, this is easily satisfied for most soils of moderate stiffness and D/t values used for large diameter piles. The soil also needs to be strong enough to sustain sufficient radial stress at the tip to cause permanent (plastic) strains in the pile, although the required (average) radial stresses reduce rapidly with increasing area of the deformed zone.

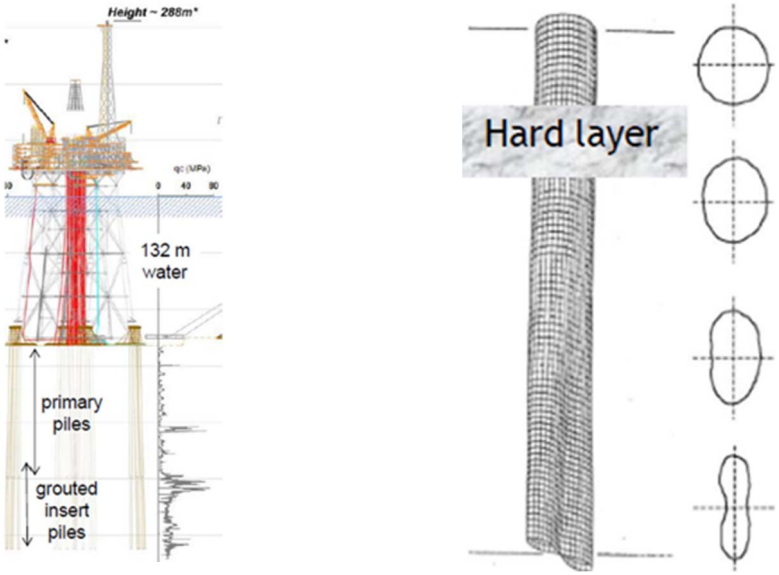

(a) Platform and foundation design (b) Measured distortion

Fig. 1. Goodwyn A platform – North-West Shelf of Australia

Embedded boulders and cemented layers are commonly associated with pile tip damage and extrusion buckling. Holeyman et al. (2015) used simplified one dimensional wave equation analyses to evaluate initiation of plastic strains in the pile due to vertical forces induced by embedded boulders. They considered the case of symmetric boulder geometry under the tip, rather than the arguably more likely situation of an eccentric boulder that would give rise to lateral denting pressure on the pile. Stevens et al. (2019) reported results of FE analysis with large boulders represented as a homogeneous hard layer to evaluate whether the pile would be distorted or the boulder would be crushed.

TESTS PLAN, SET-UP AND SAMPLE

Test plan

The centrifuge model tests reported here were performed in the 10 m diameter beam centrifuge UWA's Centre for Offshore Foundation Systems, at a model acceleration of 80g. In total, nine tests were conducted within a single soil sample, using model piles of 50 mm diameter, 0.5 mm wall thickness (D/t = 100) and 500 mm long. These were impact driven in flight into dense sand, sometimes passing through thin wedge shaped hard layers of cemented sand and gravel. Fig. 2 shows a cross section at the position where the piles penetrated the sample. The wedge shape of the hard layers was intended to cause asymmetric loading at the pile tip, which might initiate damage or slight distortion of the pile and trigger extrusion buckling. At the time of the tests, the model hammer, based on that described by De Nicola and Randolph (1994), was not able to deliver sufficient energy for the pile to penetrate, so the pile tests were concentrated towards the centre of the box, either through clean sand, or through a hard layer of maximum thickness of about 11 mm (~ $0.2D_{pile}$ or 20t). Even though a wedge shaped gravel layer was built, the pile tests conducted through it hit only a single layer of

boulders fully embedded in the dense sand. Four tests were performed through the cemented layers, two tests through the gravel layer and three tests just through clean sand. After the pile tests, a total of 10 cone penetration tests (CPTs) were conducted, spreading the tested area throughout the sample and passing through all the different layers.

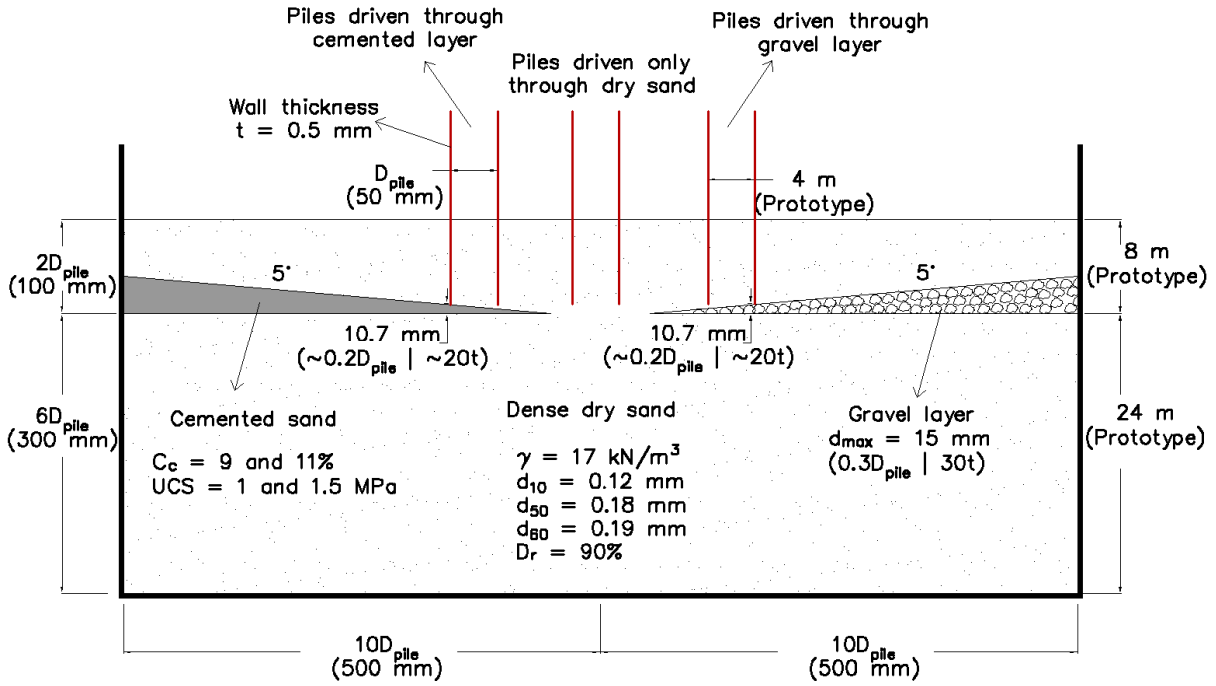

Fig. 2. Sample cross section and properties

Fig. 3 depicts the sizes of the pile wall, cone penetrometer, boulders and cemented layers. Unconfined compression (UCS) tests were performed on specimens of the same cemented materials tested in the centrifuge with different cure times to estimate the resistance of those layers.

Sample preparation

The soil sample was created without water and comprised three different materials: a) super fine silica sand; b) cemented sand; and c) gravel. The main material was superfine silica sand, which has been used extensively at COFS, with properties summarised by Chow et al. (2019). The sand has a specific gravity of 2.67 and minimum and maximum dry density of 1500 and 1770 kg/m^3. The particles are sub-rounded to sub-granular with d_{10}, d_{50} and d_{60} of 0.12, 0.17 and 0.19 mm respectively, representing a poorly graded sand (SP – USCS system). The sand layer was built using a dry pluviation technique resulting in a 90% D_r sample with dry unit weight of about 17 kN/m^3.

The cemented layers comprised a mixture of dry super fine silica sand, high early strength Portland cement and water, so classified as Special Purpose Cement Type HE, according to Australian standard AS3972 (2010). Two different cement contents were used in two quadrants of the box, Cc of 9 and 11%. UCS tests performed with curing periods from 5 to 14 days showed stabilisation of the strength after 6 days, resulting in UCS values of 1.0 and 1.5 MPa respectively. All pile tests were conducted after 7 days curing time.

The material used for the gravel comprises crushed dark granite with maximum diameter of 10 – 15 mm (0.2 – 0.3D_{pile} | 20 – 30t). The UCS of the source rock is usually around 100 – 250 MPa. This layer was also built in a wedge shape, with thickness varying from about 10 mm (single layer of aggregate) to 40 mm (4 layers of aggregate intercalated with sand) (Fig. 2),

although all the pile tests and CPTs were conducted through the single layer portion, as previously mentioned.

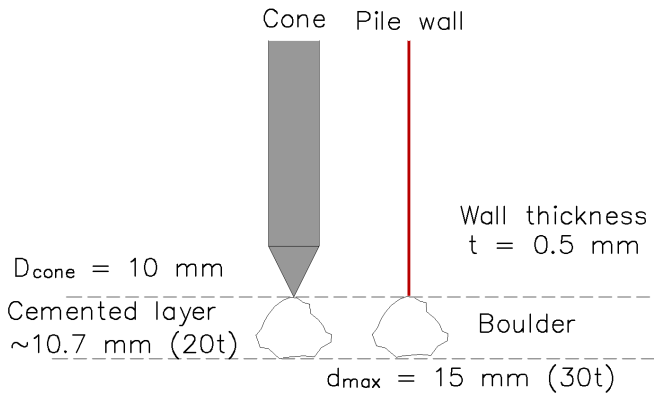

Fig. 3. Relative sizes of cone, pile, boulder and layers

Table 1. Model pile properties

Length (m)	0.5
Diameter (mm)	50
Wall thickness (mm)	0.5
D/t	100
Material	V2A-Steel (1.4301)
Young's modulus (GPa)	207
Density (ton/m^3)	7.8
Proof stress (MPa)	205

Pile and pile driving set-up

The pile driving set-up for the centrifuge tests comprised: a pneumatically operated model driving hammer; a 10 kN capacity load cell; a pile cap; a high frequency accelerometer; and live cameras for monitoring (Fig. 4).

The hammer consists of a 64 g model scale mass free falling from a maximum 16 mm drop height. At 80g the model simulates a prototype 32.8 ton hammer with maximum drop height of 1.20 m and maximum energy of 410 kJ, although with only 30% efficiency and peak force of 20 MN. The pile cap indicated in Fig. 4 was attached to the pile at the bottom and to the load cell at the top (threaded connection). A 0.8 mm thick disk of hard plastic material was placed above the load cell as a cushion, reducing the high frequency acceleration and potential accelerometer resonance.

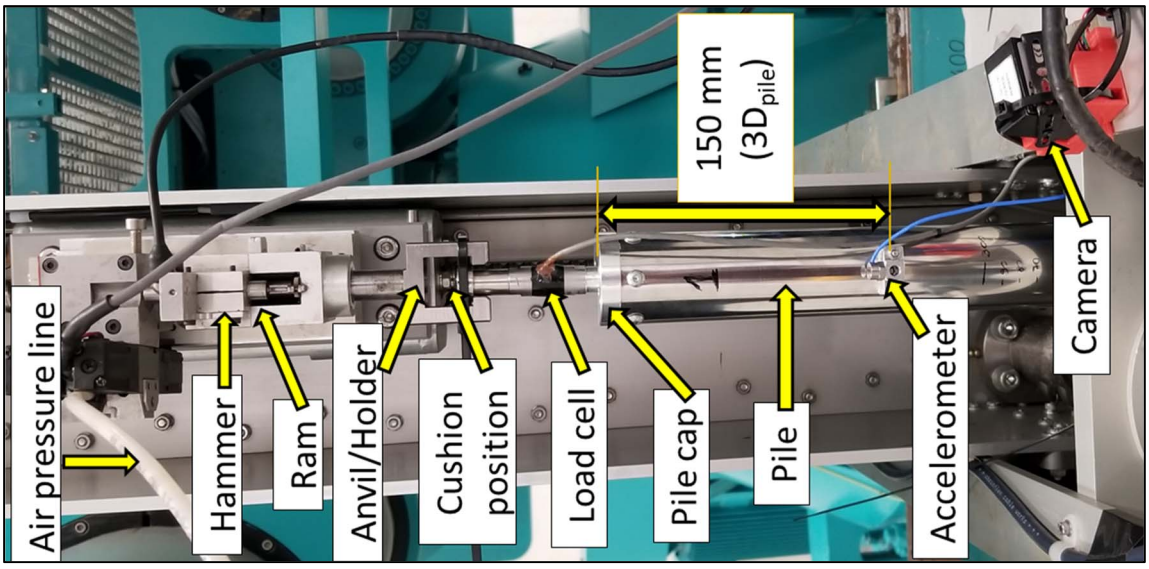

Fig. 4. Model scale pile and driving hammer

The model piles comprised 0.5 m length of stainless steel tubing (V2A-steel, N˚1.4301 - DIN EN 10088-3) with Young's modulus of 207 GPa, density of 7.8 t/m^3, yield stress of 205 MPa with 0.2% axial strain occurring for an uniaxial stress > 230 MPa. The measured external diameter averaged 50.38 mm (nominally 50 mm) representing a 4.03 m diameter prototype

pile (at 80g). The nominal wall thickness of 0.5 mm was confirmed in the range 0.51 to 0.60 (average 0.52), giving diameter to wall thickness (D/t) ratio of close to 100. The-circularity of the piles was measured ((D_{max} - D_{min})/$D_{nominal}$ ~ 0.64 - 2.7%), but the piles were found to be closely parallel relative to a central axis. All properties are summarised in Table 1.

CONE PENETRATION TESTS

The soil properties and homogeneity of the sample were investigated through cone penetration tests (CPTs). A model scale 10 mm diameter conical penetrometer was pushed into soil with a penetration rate of 1 mm/s. Spread over the tested area, four CPTs were conducted through the cemented layers (two each through the 11% Cc and 9% Cc materials), two through the gravel layer and four through just clean sand. Depth profiles of tip resistance for each test are shown in Fig. 5, where the black lines represent the tests through the cemented layers, the yellow lines through sand, and the blue lines through the gravel layer. The epoxy coating of the strain gauges just behind the cone tip was damaged twice during the tests while passing through the hard layers (CPT_{C3} and CPT_{G2}) and therefore the measured tip resistances after the damage are suspect.

A slight but clear increase of tip resistance indicates the cemented layers in CPT_{C1} and CPT_{C2}. Even though the cone was damaged during CPT_{C3} the signal was not lost until 225 mm penetration. The damage probably occurred during penetration of the cemented layer, so the cone resistance below that must be considered with caution even though the trend of the curve looks reasonable.

The increase in cone resistance is less evident in the gravel layer, with CPT_{G1} showing a slight change but no sharp increase and CPT_{G2} an initial increase near the gravel layer followed by an abrupt decrease. The decrease and subsequent values are suspect as the cone was found to be damaged after the test and the damage probably happened when passing through the gravel layer. The CPTs in sand alone (CPT_{S1-4}) show very good agreement, especially in the upper 100 mm. Below that depth, CPT_{S1} falls below the close grouping of the other three tests.

Overall, the tests revealed a quite homogenous 90% D_r sand sample, especially for the first 100 mm, with q_c increasing from zero at the surface to about 50-70 MPa at 200 mm depth ($4D_{pile}$ = 16 m). A slight increase on the cone resistance due to the presence of the cemented layers was evident, but any increase was much smaller for the gravel layer. Both hard layers ended up damaging the cone, showing the potential for triggering pile tip damage.

PILE DRIVING TESTS

Pile tests

Nine pile driving tests were conducted across the sample, either down the centreline (sand only) or through one of the hard layers (Fig. 2). The cumulative blowcounts are presented in Fig. 6. Also, for every pile test, acceleration and force measurements were made for two or three blows during penetration in order to estimate the delivered hammer energy. The test numbers indicate the order of each new model pile, but some piles (P1C, $P4_{2nd}$, P5C) were driven a second time, as explained below.

The tests started with P1 being driven through a ~10 mm thick 9% C_c layer (Fig. 6). After some difficulty in passing through the cemented layer (~90-100 mm depth), the test continued and the pile reached 127 mm. When extracted, a plug made of cemented material was found 23 mm from the tip and a very small dent (0.44 mm – 0.87% of D_{pile} – 0.88t) was found (Fig. 7a).The second test was P2, where the pile was supposed to be driven through the ~10 mm thick part of the 11% C_c layer. However, it reached refusal at 96 mm penetration, about 6 mm into the hard layer and the test was stopped after 5,000 blows. When the pile was extracted, no damage on the tip was observed.

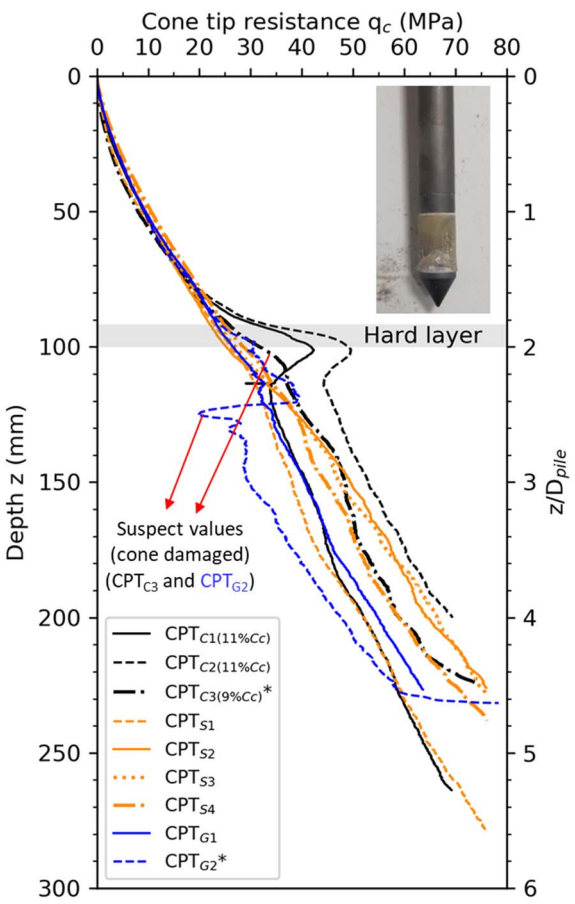

Fig. 5. Profiles of cone resistance

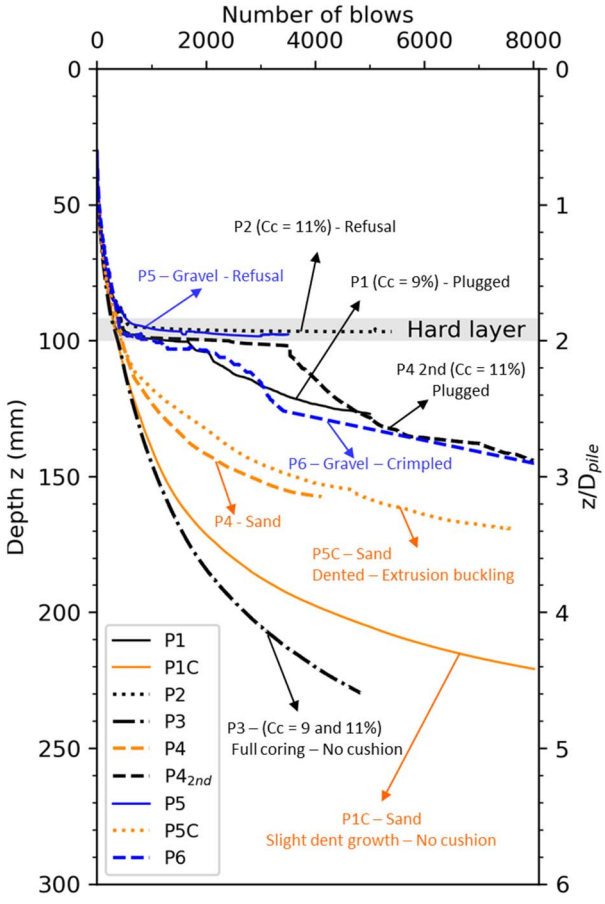

Fig. 6. Pile driving blowcount profiles

Black lines – tests through cemented layer. Orange lines– tests just through sand. Blue lines – tests through gravel layer

In an attempt to simulate an extreme case, where half of pile would penetrate through the ~10 mm thick part of the 11% C_c and half would penetrate just sand, test P4 was conducted. The test ended up missing the hard layer and being conducted only through sand. This test became a reference case in just clean sand. The same undamaged pile was extracted and moved towards the cemented layer in a new attempt. Test $P4_{2nd}$ ended up with the pile penetrating fully through the cemented layer, using a process of alternately driving and jacking in order to progress the penetration. The pile advanced to a depth of 140 mm after 8,000 blows, but no damage was observed at the pile tip after extraction.

Test P5 was the first undertaken through the gravel layer (~10 mm thick), but the pile refused near the base of the hard stratum (100 mm depth). A dent of maximum depth 0.9 mm (1.8% D_{pile}, 1.8t) was found at the pile tip (Fig. 7b). The dent had a similar rounded triangular shape to that in Test P1, though double the size with the apex ~12 mm from the tip.

A second test, P6, was conducted through the gravel and passed through the 10 mm thick layer, by means of a jacking and driving process, to a depth of 110 mm. From that point the pile continued to be impact driven and, despite evident hard driving response, eventually reached 140 mm depth. When extracted, severe damage was found at the tip, extending 17 mm up the pile (Fig. 7c). A sample survey carried out after the tests revealed a single boulder at 117 mm depth, 17 mm below the original hard layer. This information suggests the boulder was pushed 17 mm by the pile in the process of being pushed to one side.

At this stage, the hard layers had showed potential for triggering pile tip damage (Fig. 7a, b and c). However, the low hammer energy proved insufficient to permit penetration sufficiently below the hard layer to demonstrate extrusion buckling. For the cemented layer, the presence

of solid plugs of the cemented material may have provided sufficient resistance inside the pile. To explore extrusion buckling further, the pre-dented piles 1 and 5 were re-driven just through clean sand in the central strip of the box.

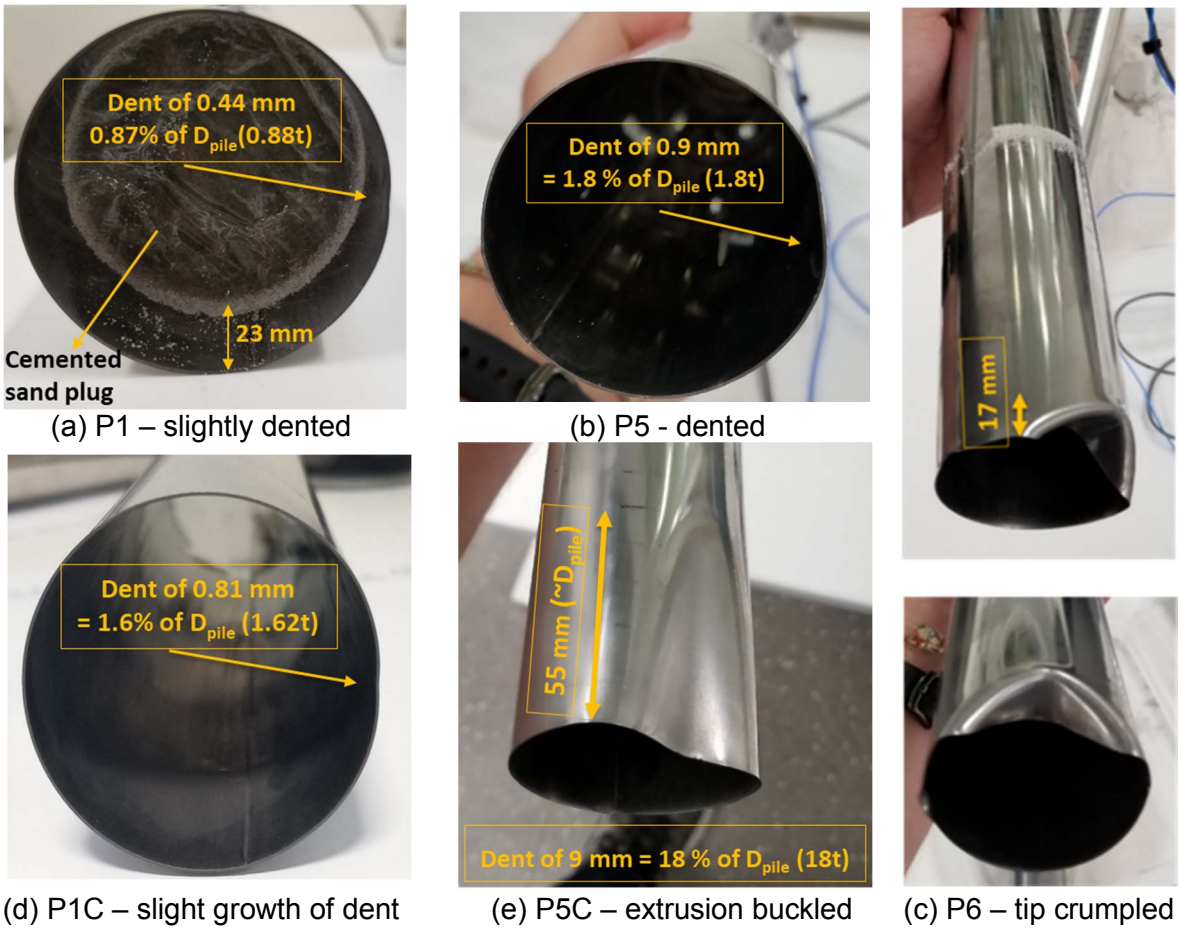

(a) P1 – slightly dented (b) P5 - dented

(d) P1C – slight growth of dent (e) P5C – extrusion buckled (c) P6 – tip crumpled

Fig. 7. Details of tip damage and extrusion buckling

Firstly P5 was re-driven just in sand, with the test referred to as P5C in Fig. 6. The test reached a penetration of 170 mm after almost 8,000 blows, showing much harder driving below a depth of 100 mm compared with test P4 driven just through sand. After extracting the pile from the soil it was seen that the initial dent had increased significantly, with the pile having undergone extrusion buckling. Later measurements revealed a 9 mm dent (18% of D_{pile}) extending 55 mm from the pile tip in a classical extrusion buckling shape (Fig. 7e).

Test P1C was then conducted by driving the slightly damaged pile 1 also just through sand trying to reproduce the results from P5C. To reach a deeper penetration, and therefore higher pressures, the cushion on the pile cap was removed, which increased the hammer energy by an estimated 30% (from the peak force). However, the absence of the cushion prevented consistent stress-wave measurements due to high frequency vibration caused by the steel-to-steel contact. The higher peak force and energy allowed the pile to penetrate deeper in the soil, showing easier driving compared with the earlier tests. The test proceeded to a depth of 217 mm with 8,000 blows. The pile was then extracted from the soil and later measurements revealed a slightly increased dent (0.81 mm – 1.6% of D_{pile} – compared with 0.44 mm initially) extending 10 mm from the tip (Fig. 7d).

Still without any cushion, the last test was P3, where the pile was driven between the two cemented materials (9 and 11% Cc) where there was a 20 mm gap filled with sand (due to the use of a plywood separator during casting the layers). Driving the pile at this location should

avoid the formation of a plug that would limit further penetration, and also might cause some damage at the pile tip during penetration through the cemented layers. The pile was penetrated to 230 mm depth with 8,000 blows, having been stopped once due to signs of damage to the hammer. When the pile was extracted, neither cement plug nor tip damage was evident.

Overall behaviour

The blowcount curves for all piles in Fig. 6 can be divided in three groups with distinct behaviour: (i) a band of effectively plugged driving responses; (ii) a band of unplugged response but with higher energy (following removal of the hammer cushion); and (iii) intermediate driving response.

The first group is formed by tests P1, P2, $P4_{2nd}$, P5 and P6 in which all piles had a plugged behaviour. P2 and P5 met refusal within the 11% cement and gravel layers respectively, unable to be penetrated further. Both P1 and $P4_{2nd}$ passed through the cemented layers (9 and 11% cement respectively) and formed a solid plug with the material. $P4_{2nd}$ had more difficulty in passing through the hard layer, relying on an iterative driving and jacking procedure to succeed. Nevertheless, after breaking through, the pile eventually penetrated more than P1 because of the greater number of blows applied. Likewise, P6 passed through the gravel layer, relying on driving and jacking; however, the tip had by that stage partially crumpled (see Fig. 7 c), so the hard driving reflects the resulting high end bearing resistance.

The second group is formed by tests P1C and P3. Both tests were conducted with higher energy, due to the absence of the cushion, and exhibited non-plugged behaviour. P1C had a small initial dent that grew slightly during the test, although insufficiently to increase significantly the driving resistance. Even though P3 intersected both the 9 and 11% cement materials, no plug was formed as the test was conducted in line with a sand-filled central gap between the two cemented zones. The difference between the two curves may be attributed to soil variability.

The third group comprises Tests P4 and P5C. Both tests were conducted just through sand, with the cushion and initially non-plugged behaviour. P4 reached a depth of 160 mm while P5C reached 170 mm, but with clearly harder driving. As discussed earlier, P5C suffered extrusion buckling, triggered by an initial dent, and distorted considerably; this led to increased driving resistance near the pile tip. On the other hand, P4 remained undistorted but driving was stopped at a similar depth because of the high blow rates. During jacked pile penetration in dense sand, a plug starts to develop beyond a penetration of about $3D_{pile}$ (Fan et al. 2020). Even during driving, with relatively low delivered energy, penetration beyond that depth is likely to exhibit partial plugging (i.e. an incremental filling ratio less than that for fully unplugged penetration). The relatively similar driving responses of tests P4 and P5C, both of which had similar delivered hammer energy, confirms the likely partially plugged behaviour of P4.

Although both hard layer types were able to initiate tip distortion, the boulder layer was found to cause more damage. The gravels caused a marked dent during test P5 and severe tip crumpling in test P6, while the cemented layer only caused a very small dent in one pile, P1. This may be attributed to the high hardness and angularity of the aggregate material, causing a severe ‘point’ like contact with the pile rather than a more distributed one in the cemented layer.

PILE TIP DAMAGE AND EXTRUSION BUCKLING

To understand the conditions where extrusion buckling occurred for test P5C, it may be noted from Fig. 6 that the blowcount for test P5C started to deviate from the other two piles in sand (P4C and P1) at approximately 95 mm depth. A sample ‘exhumation’ performed after the pile tests, where the soil was carefully excavated to reveal evidence of the pile locations, confirmed

this. An already distorted shape 'footprint' of P5C was found at 106 mm depth. The tip resistance (q_c) at 90-95 mm depth, where extrusion buckling would have been initiated, was around 24-26 MPa. This indicates the sand strength (and stiffness) required to start increasing the initial dent of 0.9 mm (1.8 % of D_{pile}) appreciably, eventually reaching 9 mm, and extending 55 mm ($1.1D_{pile}$) from the tip, by a depth of 170 mm (further penetration of ~$1.6D_{pile}$).

Even though minor dent growth occurred in test P1C, there is no corresponding evidence from the blowcount curves. The initial dent of 0.41 mm (0.87 % of D_{pile}) that occurred when P1 was driven through the 9% cement layer grew slightly to 0.81 mm (1.6 % of D_{pile}) during re-driving in sand alone to a final depth of 240 mm (4.8 D_{pile}).

For test P6, where the pile tip crumpled after passing through the gravel layer, the blowcount curve in Fig. 6 suggests that severe tip closure occurred by a depth of around 125 mm, but probably occurred as the pile tip advanced from 110 mm to 125 mm, with q_c of 25-35 MPa.

CONCLUSIONS

The centrifuge model tests reported here have demonstrated a range of tip damage that can occur as a steel pile with D/t of 100 is driven into dense sand containing a hard layer. The main conclusions are:

1. Driving through a layer of single 'boulders' of dimension 0.2-0.3D_{pile} (20-30t) results in greater damage than driving through a (simulated) uniformly cemented layer of 0.2D_{pile} (20t) thick.
2. Tip damage from a boulder layer ranged between a moderate dent (1.8% of D_{pile} | 18t) to triggering severe tip crumpling as the pile advanced by ~0.3D_{pile}.
3. A slight initial dent of the pile tip can lead to extrusion buckling when the pile is driven into dense sand, with the severity of the increased tip distortion a function of the initial dent size and the cone resistance. In these tests, q_c exceeding 25 MPa was required to cause further tip distortion.

REFERENCES

Aldridge, T.R. Carrington, T.M. & Kee, N.R. (2005). Propagation of pile tip damage during installation. Proc. of International Symposium on Offshore Geotechnics, Perth, Taylor & Francis, 823-827.

Alm, T., Snell, R.O., Hampson, K.M. & Olaussen, A. (2004). Design and installation of the Valhall piggyback structures. Proc. Offshore Tech. Conf., Houston, Paper OTC 16294.

API. (2002). Recommended practice for planning, designing, and constructing, fixed offshore platforms – Working stress design, API RP2A 21st edition December 2000, Errata and Supplement December 2002, American Petroleum Institute, Washington.

Bakroon, M., Daryaei, R., Aubram, D., & Rackwitz, F. (2018). Numerical evaluation of buckling in steel pipe piles during vibratory installation. Soil Dynamics and Earthquake Engineering.

Barbour, R. & Erbrich, C.T. (1995). Analysis of soil skirt interaction during installation of bucket foundations using ABAQUS. Proc. ABAQUS Users Conference, Paris.

Barbour, R.J. & Erbrich, C. (1994). Analysis of in-situ reformation of flattened large diameter foundation piles using ABAQUS. Proc. UKABAQUS Users Conference, Oxford.

Bresse, J. A. C. (1866). Cours de mecanique appliquee par M. Bresse: Hydraulique (Vol. 2). Mallet-Bachelier.

Chow, S.H., Roy, A., Herduin, M., Heins, E., King, L., Bienen, B., O'Loughlin, C.D., Gaudin, C. & Cassidy, M.J. (2019). Characterisation of UWA superfine silica sand, Report GEO 18844, Centre for Offshore Foundation Systems, Perth, Australia.

De Nicola, A. & Randolph, M.F. (1994). Development of a miniature pile driving actuator. Proc. Int. Conf. Centrifuge '94, Singapore, Balkema, Rotterdam, 473-478.

DIN EN 10088-3: Nichtrostende Stähle – Teil 3: Technische Lieferbedingungen für Halbzeug, Stäbe, Walzdraht, gezogenen Draht, Profile und Blankstahlerzeugnisse aus korrosionsbeständigen Stählen für allgemeine Verwendung, Beuth Verlag, Berlin, Germany (2014)

Ellinas, C.P., Walker, A.C., 1983. Damage Offshore Tubular Bracing Members. pp. 253–261.

Erbrich, C.T., Barbosa-Cruz, E. & Barbour, R. (2010). Soil-pile interaction during extrusion of an initially deformed pile. Proc. 2nd Int. Symp on Offshore Geotechnics, Perth, 489-494, Taylor & Francis, London.

Erbrich, C.T., Lam, S.Y., Zhu, H., Derache, A., Sato, A. & Al-Showaiter, A. (2017). Geotechnical design of anchor piles for Ichthys CPF and FPSO. Proc. 8th Int. Conf. Offshore Site Investigation and Geotech., Society for Underwater Technology, London, 2, 1186-1197.

Fan, S., Bienen, B. & Randolph, M.F. 2020. Effects of pile installation on subsequent response under lateral loading, Part I: Pile installation. Under review.

Finnie, I.M., Gillinder, R., Richardson, M. Erbrich, C.J., Wilson, M., Chow, F., Banimahd, M. & Tyler, S. (2019). Design and installation of mobile offshore drilling unit mooring piles using innovative drive-drill-drive techniques. Proc. 13th Australia-New Zealand Conf. on Geomechanics, Perth.

Health and Safety Executive. (2001). A study of pile fatigue during driving and in-service and of pile tip integrity. Offshore Technology Report, 2001/018.

Holeyman, A., Peralta, P., & Charue, N. (2015). Boulder-soil-pile dynamic interaction. In Frontiers in Offshore Geotechnics III: Proc. 3rd Int. Symp. on Frontiers in Offshore Geotechnics (ISFOG 2015), 1, 563-568, Taylor & Francis, London.

Kramer, G. (1996). Investigation of the Collapse Mechanism of Open Ended Piles during Installation. Masters Thesis, Technical University of Delft.

Standards Australia, 2010. AS 3972-2010 General Purpose and Blended Cements. Sydney: Standard Australia.

Stevens, R. F., Westgate, Z., & Kocijan, J. 2019. Assessing the Pile Driving Risk Due to the Presence of Boulders. Proc. Offshore Tech. Conf., Houston, OTC 29668.

Stevens, R.S., Wiltsie, E.A. & Turton, T.H. 1982. Evaluating pile drivability for hard clay, very dense sand, and rock. Proc. Offshore Tech. Conf., Houston, OTC 4205.

Wiltsie, E.A., Stevens, R.F. & Vines, W.R. 1985. Pile installation acceptance in strong soils. Proc. 2nd Int. Conf. on Application of Stress Wave Theory to Piles, Stockholm, 72-78.

Timoshenko, S. P., & Gere, J. M. (1961). Theory of elastic stability. McGraw-Hill, New York.